Polymer Bulletin 61, 353–362 (2008)
DOI 10.1007/s00289-008-0956-0

Polymer Bulletin

The Influence of the compatibilizer Characteristics on the interfacial characteristics and phase morphology of aPA/SAN blends

Daniela Becker, Fernanda Porcel, Elias Hage Jr. and Luiz A. Pessan (✉)

Universidade Federal de São Carlos - UFSCar
Programa de Pós-Graduação em Ciência e Engenharia de Materiais - PPG-CEM

E-mail: pessan@power.ufscar.br

Received: 18 December 2007 / Revised version: 28 March 2008 / Accepted: 27 May 2008
Published online: 10 June 2008 –

Summary

The main objective of this work is study the influence of the methyl mathacrylate maleic anhydride copolymer (MMA-MA) compatibilizer properties such as molecular weight and maleic anhydride content in the characteristics of amorphous polyamide and styrene acrylonitrile copolymer (aPA/SAN) blends, correlating their interfacial characteristics and phase morphology. The blends aPA/SAN, with and without the compatibilizer, prepared were characterized by transmission electron microscopy (TEM) and small angle X-rays scattering (SAXS). The results show that the maleic anhydride concentration has a more significant effect on the blend properties than the molecular weight of the MMA-MA copolymer. Even though the system aPA/SAN is thermodynamically immiscible, it shows morphology of phases with small particles of SAN. The addition of MMA-MA copolymer with high degrees of MA led to an increase of the SAN phase particle size. With SAXS technique, it was possible to determine the interface thickness and the results shows that the characteristics of the interface do not change with the variation of the compatibilizer characteristics. The results observed in this work indicate that the viscosity ratio is very important factor on the formation of the phase morphology.

Introduction

The reactive compatibilization technique, through which potentially reactive copolymers or functionalized polymers are added to polymer mixtures, have proved to be an effective method to control and stabilize the phase morphology and improve the mechanical properties of polymer systems. The compatibilizer copolymer reduces the interfacial tension between the components of the blend and inhibits the coalescence of the disperse phase, and therefore, promoting an adequate morphology of phases as well as its stabilization. Also, the compatibilizer might improve the interfacial adhesion between the components of the blend and reduce the possibilities of interfacial failure [1,2].

Maleic anhydride (MA) modified polymers are often used as compatibilizers in blends with polyamide due to the high probability of chemical reaction between MA functional unities and the amine end-groups of polyamide (PA) during melt blending [3-6]. This reaction is expected to occur fast and results in imide linkage formation, as shown in Figure 1. This same behavior is observed in blends with amorphous polyamide [7-8]. Methyl methacrylate based copolymers are miscible with acrylonitrile-styrene copolymer (SAN) copolymer for a wide range of acrylonitrile (AN) content, and therefore, the MMA-MA copolymers are very promising in compatibilizing polyamide and SAN based polymers blends [9].

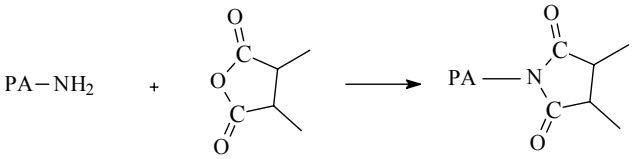

Figure 1. Scheme of interface grafting by reaction between a carboxyl group of maleic anhydride and a polyamide amino end group.

When selecting a compatibilizer for a specific polymer blend, one should take into account several factors such as: the molecular architecture, the chemical composition and the molecular weight of the copolymer. Larocca et al [10] observed, through viscosity and morphological analysis, that, in blends of poly(butylene terephthalate), acrylonitrile-ethylene-propylene-diene-styrene and methyl methacrylate/glycidyl methacrylate/ethyl acrylate terpolymers as compatibilizer, PBT/AES/MGE, the effect of the compatibilizer is more significant when addeing MGE with lower molecular weight.

The objective of this work is to study the influence of the MMA-MA compatibilizer characteristics, such as molecular weight and maleic anhydride content, on aPA/SAN blends correlating the interface and phase morphology characteristics. These properties were investigated using transmission electron microscopy (TEM) and small angle X-rays scattering (SAXS).

Experimental

Materials

The amorphous polyamide used was supplied by Dupont under the trade name SELAR PA 3426, chemical structure is illustrated in Figure 2 and the SAN copolymer was provided by Dow Chemical as Tyrill 790, the characteristics of these materials are shown in Table 1. The reactive compatibilizer used was the methyl metacrylate and maleic anhydride copolymer (MMA-MA) synthesized in our laboratories.

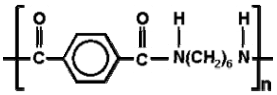

Figure 2. Chemical structure of amorphous polyamide

Table 1. Characteristics of the used materials

Materials	Description	Composition	Molecular weight (g/mol)	Tg (°C)
aPA	SelarPA 3426	End group content: [NH2] 37 μeq g -1	$\overline{M}_n$=12,000 $\overline{M}_w$= 47,000	127
SAN	Tyrill 790	S = 72% AN = 28%	$\overline{M}_n$= 61,028 $\overline{M}_w$= 136,756	110

The MMA and MA monomers used in the synthesis of the MMA-MA copolymer were supplied by Metacril and Aldrich, respectively. The copolymers were synthesized with 1, 5 and 10% of maleic anhydride, using toluene as solvent. To control the molecular weight, benzoil peroxide was used as initiator in different amounts. The desired amounts of each monomer, initiator, solvent and also 2% of ethyl acrylate (added to prevent the unzipping degradation at processing temperatures) were added in a reactor and kept at 80°C for 8 hours under stirring. The procedure for the synthesis of MMA-MA is based on work reported in the literature [11] and its details are given elsewhere [12]. Table 2 shows the synthesized copolymers and their characteristics.

Table 2. MMA-MA copolymers and their characteristics

Copolymer	%MA*	Mw**	Mw/Mn
MMA-MA0 HMW	-	55,924	1.78
MMA-MA1 HMW	1.08±0,02	52,380	1.61
MMA-MA5 HMW	5.00±0,08	57,474	1.95
MMA-MA10 HMW	9.80 ± 0,40	60,365	2.57
MMA-MA1 MMW	0.83±0,06	34,217	1.73
MMA-MA5 MMW	5.14±0,10	33,782	1.75
MMA-MA10 MMW	8.97±0,21	42,839	2.73
MMA-MA1 LMW	0.74±0,03	22,895	1.85
MMA-MA5 LMW	5.97±0,17	25,185	2.71
MMA-MA10 LMW	8.27±0,37	22,643	2.80

* determined by titration [6]; ** determined by GPC [6]

Preparation of the blends

The binary aPA/SAN (80/20) and the ternary aPA/SAN/MMA-MA (76/19/5) mixtures were prepared in a Werner & Pfleiderer ZSK-30 co-rotating twin-screw extruder. Before the extrusion process, the materials were dried for 3 days at 60°C in air-circulating oven and for 48 hours at 80°C in vacuum oven. The rotation of the screws was set to 150 rpm and the material feeding rate to 3 kg/h. The temperature profile of the extruder's heating zones was: 195°C (feeding zone)/264°C/265°C/260°C/260°C/260°C.

After the extrusion, the mixtures were injection molded into an ARBURG 270V injection molding machine. ASTM D-638 tensile test specimens were made. The temperature profile used in the injection molding process was in the range of 220-250°C, the mold temperature was 80°C and the cooling time was 40 s.

Morphological Characterization

The morphology of the blends was observed through transmission electron microscopy (TEM), using a Jeol 100CX microscope, operating at 80 kV of accelerating voltage.
The samples analyzed by TEM were taken from the injection molded tensile test specimen. The observed area was located at an intermediary position of thickness and length of the sample and in the direction perpendicular to the injection flow. The samples were stained by immersion in a 10% phosphotungstic acid (PTA) aqueous solution for 6 days, when the substance etches preferably the polyamide phase. After that, the samples were microtomed, i.e., cut into ultra-thin sections with nominal thickness of 20 nm on a Leica ultramicrotome using a diamond knife at room temperature. The slices of the polymer samples floating in water both in the ultramicrotome were collected with cooper grids.

Small Angle X-ray Scattering (SAXS)

Small Angle X-ray Scattering (SAXS) measurements were performed to estimate the thickness of the interface formed between the phases in the aPA/SAN/MMA-MA blends. The SAXS measurements were made at the Laboratorio Nacional de Luz Sincrontron (LNLS) in Campinas – Brazil. A one-dimensional gas detector, sensible to the position and beams of 1.608 Å of wavelength was used. The sample to detector distance used was of 545.8 mm. Samples for SAXS were obtained from the injection molded tensile specimens, by reducing their thickness to 1 mm using sandpapers with numbers 80,120,240,400 and 600. The SAXS results were obtained by two kinds of measurements. In the first it was used a slit of 1 mm during 5 minutes to get a complete spectrum. In the second one it was used a slit of 8 mm, closed with 2.5 mm of lead band, for 20 minutes to get the spectrum near the Porod region. All measurements were made in duplicates.

Results and Discussion

Figure 3 shows the TEM micrographies of the injected molded aPA/SAN/MMA-MA blends. It is observed for the uncompatibilized blend (Figure 3(a)) a structure with disperse phase of heterogeneous size. The use of the compatibilizer with 1% of maleic anhydride apparently led to a structure with a better dispersion, Figure 3 (b)-(d). The use of a compatibilizer with 1% of maleic anhydride with different molecular weight led to a small change on the phase morphology. The addition of compatibilizer with higher amounts of maleic anhydride (5 and 10%) led to an increase of the particle size and to a more heterogeneous structure (Figure 3 (e)-(j)). The blends with MMA-MA5 (Figure 3(e)-(g)) showed an unstable structure with very elongated disperse phase, indicating an intermediary structure. The blend with MMA-MA5 LMW (Figure 3(j)) showed a smaller disperse phase size than the other blends with 5% of MA. For the blends with MMA-MA10 (Figure 3(h) – (j)), though, the change in molecular weight did not apparently led to significant changes on the morphology.
A possible reason for the increase on particle size with the addition of the compatibilizer with higher amounts of maleic anhydride (5 and 10%) is the fact that the blends with compatibilizer show a significant increase in their melt viscosity when compared to the corresponding uncompatibilized system, changing the viscosity ration

between the components ratio [13,14]. Favis et al [15] observed lower and higher limits to the viscosity ratio between the disperse phase and matrix (η_d/η_m) in PP/PC blends, out of which the deformation and break-up of the particles become more difficult. For high viscosity ratios, the viscous forces that cause the break-up of the particles do not overcome the interfacial forces of the disperse phase and therefore the particles will not break-up. On the other hand, conditions of very low viscosity ratios, will cause high deformation of the disperse particles, however they will not break.

Literature shows [3-8] that reactions occur between the maleic anhydride and the amine end groups of the amorphous polyamide, leading then to the formation in situ of aPA-g-MMA-MA copolymer. The torque ratio between the SAN and the aPA/ MMA-MA materials at 2 minutes of mixing time in a internal rheometer Haake was determined, and the data is shown in Table 3. It can be observed that the mixture between aPA and MMA-MA copolymer have a high viscosity when compared to neat aPA and, consequently, shows a reduction of the torque ratio of the system based on aPA and SAN. When the torque ratio becomes much lower than 1, the particle size increase. On the other hand, the effect of the compatibilizer should reduce the interfacial tension, and also to the formation of smaller dispersed particles of SAN. It was observed in this work that the addition of acrylic copolymers MMA-MA to the aPA/SAN blend may cause both effects. The size of the SAN disperse phase increase with torque ratio however it should be noted that η_d/η_m is still too small and much lower than 1, between 0.1 and 0.6. The addition of the lower molecular weight com-

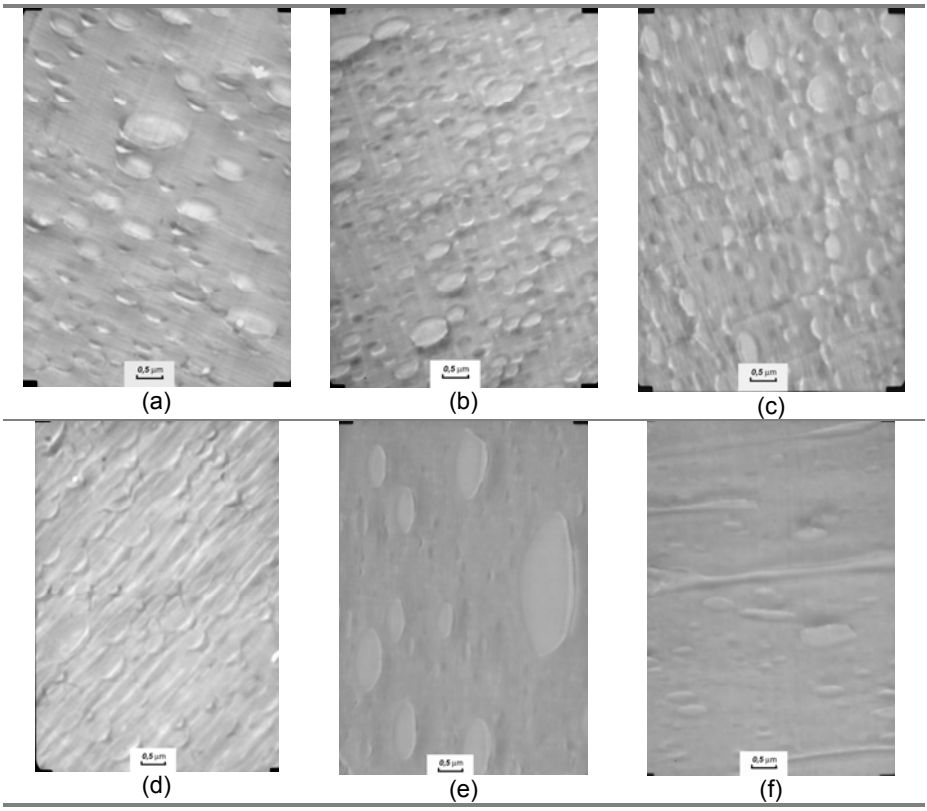

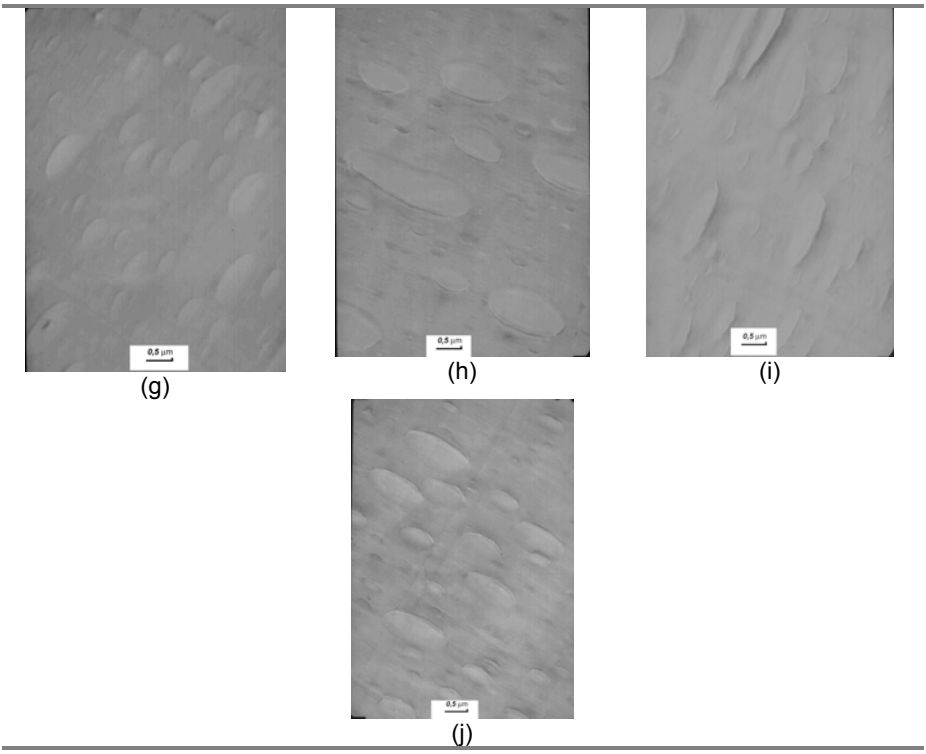

Figure 3. TEM Micrographies of the injection moulded blends: (a) PA/SAN; (b)aPA/SAN/MMA-MA1 HMW; (c) aPA/SAN/MMA-MA1 MMW; (d) aPA/SAN/MMA-MA1 LMW; (e) aPA/SAN/MMA-MA5 HMW; (f) aPA/SAN/MMA-MA5 MMW; (g) aPA/SAN/MMA-MA 5 LMW; (h) aPA/SAN/MMA-MA10 HMW; (i) aPA/SAN/MMA-MA10 MMW; (j) aPA/SAN/MMA-MA10 LMW.

Table 3. Torque ratio of aPA/SAN/MMA-MA blends at 260°C

Samples	Torque at 2min. (N.m)*	Torque ratio [SAN/(aPA/MMA-MA)]
SAN	1.9	-
aPA	2.4	0.8
aPA/MMA-MA1 HMW	3.7	0.5
aPA/MMA-MA5 HMW	3.8	0.5
aPA/MMA-MA10 HMW	3.7	0.5
aPA/MMA-MA1 MMW	6.5	0.3
aPA/MMA-MA5 MMW	10.0	0.2
aPA/MMA-MA10 MMW	8.3	0.2
aPA/MMA-MA1 LMW	9.2	0.2
aPA/MMA-MA5 LMW	11.2	0.2
aPA/MMA-MA10 LMW	9.2	0.2

* mixing time in a internal mixer Haake

patibilizers show more significant increase on the SAN's particle size, what can be related to the high molecular mobility of these copolymers, allowing a higher

extension of grafting reactions during the 2 minutes of processing, as indicated by the torque measurements.

Determination of the interface thickness by SAXS

SAXS is a useful method for estimating interfacial thickness. In this section, the results of interfacial thickness obtained from Porod analysis will be discussed. Porod analysis is generally performed in the region of final slope of the scattered intensity [16,17]. The final slope of the scattering curve implies the high-s region of the small-angle scattering profile.
SAXS curves for the blends containing the compatibilizer with high molecular weight are shown in Figure 4, where s as the scattering vector,

$$s = 2\text{sen}\theta/\lambda \quad (\mathbf{1})$$

where θ is the half of the scattering angle and λ is the wavelength (λ=1.608 Å). The behavior illustrated in the figure is similar to the one observed for the other blends.
To eliminate the positive deviations present on the measurements, the Vonk method was used [18].

$$I_{back}(s) = A + Bs^n \quad (\mathbf{2})$$

Where A and B are constants and n=2,4,6 … Is an adjustable parameter
To all the blends, the background intensity is best describe with n = 4, in spite of the compatibilizer characteristics. The graphic I(s) vs s^4 shows a straight line, as seen on Figure 5(a) for the aPA/SAN/MMA-MA1HMW blend. Through curve adjustments, it is possible to observe that the Vonk empirical method adjusts efficiently in regions of high angles of the scattering curve, Figure 5(b). A similar behavior was observed for all the other blends. The subtraction of the background intensity can therefore be performed, and the resulting scattered intensity can be used to evaluate the interfacial thickness.
To determine the interface thickness, Porod's Law relation was used [19],

$$I_{corr}(s) = K_p / s^4 \exp\left(-4\pi^2\sigma^2 s^2\right) \quad (\mathbf{3})$$

where $I_{corr}(s) = I - I_{back}$, Kp is the Porod constant, s is the magnitude of scattering vector. Suitable plots of its equation allow the determination of σ. In this paper, $E=(12\sigma)^{1/2}$ will be taken as measurement of the interfacial thickness. A plot of $\ln(I_{corr}s^4)$ vs s^2 should show a linear region of negative deviation at high s where by adjusting the better curve the angular coefficient is used to determine the interface thickness.
Figure 6 there shows a correlation between $\ln(Ic_{orr}s^4)$ vs. s^2 for the aPA/SAN/MMA-MA1HMW blend with indication of the region in with the adjustment, and a linear fitting at high-s region are given, this linear fit was used for estimation of the interfacial thickness of this sample (E=2.60 ±0.14), using equation 3. It is important to mention that in all curves the negative inclination region, although short, is easily identified. Besides that, after the elimination of the background scattering intensity, there is a shortening on the scattering vector region, because at high values of s, the background intensity overtakes it. All of the results pertaining to the interfacial thickness from Porod analysis are summarized in Table 4.

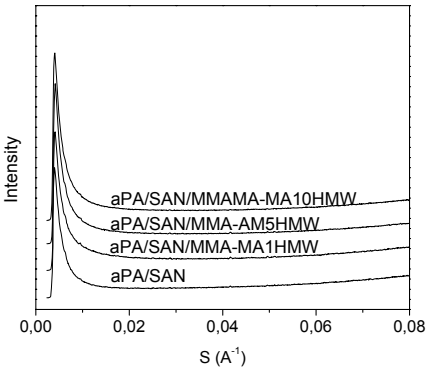

Figure 4. Small-angle X-ray scattering curves for aPA/SAN/MMA-MA blends

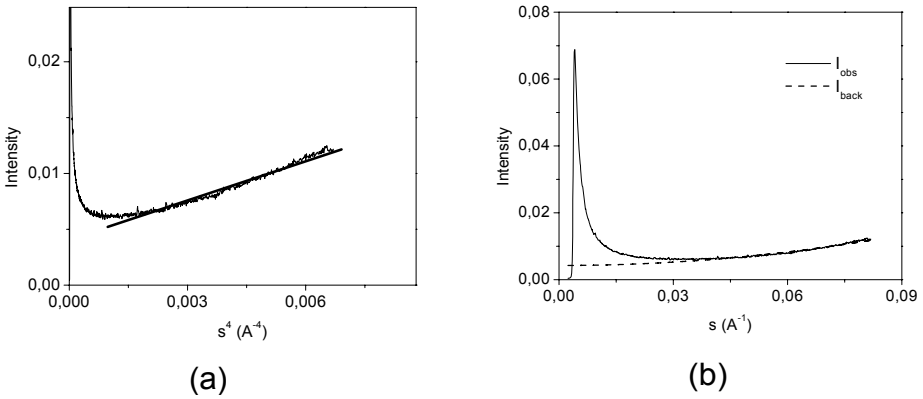

Figure 5. (a) Determination of background intensity by Vonk empirical method for aPA/SAN/ MMA-MA1HMW blends; (b) Observed intensity and background intensity determined by Vonk empirical method for aPA/SAN/MMA-MA1HMW blends.

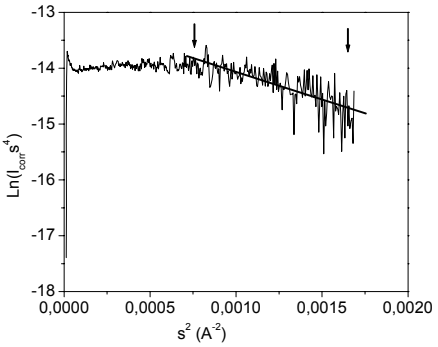

Figure 6. Porod plot in the form of $\ln(I_{corr}s^4)$ as function of s^2 for aPA/SAN/MMA-MA1HMW blends

In Table 4 can be observed that there is no significant change of the interface thickness values with the variation of characteristics of the compatibilizer, indicating that

the molecular weight as well as the compatibilizer maleic anhydride content does not affect significantly the interactions at the interface for this system. It was not possible to determine the interface thickness for the uncompatibilized blend. There are two possible reasons for this. The method used for the calculations is not adequate for this system or that the thickness is below the detection limit for the technique used. Therefore, the results of this work leads to the concluion that the addition of the compatibilizer MMA-MA to the system aPA/SAN, independent of the compatibilizer characteristics, increases the interface thickness as compared to the uncompatibilized blend. This behavior correlates well with the morphologies observed for these systems with TEM, indicating that the viscosity ration between the blends components is the main factor responsible by the formation of the phase morphology of the blends studied. Also, the interfacial tension may not be influenced by the compatibilizer characteristics studied in this work, such as the molecular weight and the amount of maleic anhydride. Apparently, the addition of compatibilizer leads to the formation of interphase in the system studied compared to the uncompatibilized blend did not show the characteristics related to interface presence.

Table 4. Interfacial thickness of aPA/SAN blends determined by SAXS

Sample	Interfacial thickness (nm)
aPA/SAN	-
aPA/SAN/MMA-MA1 HMW	2.60 ±0.14
aPA/SAN/MMA-MA5 HMW	2.75±0.21
aPA/SAN/MMA-MA10 HMW	2.95±0.07
aPA/SAN/MMA-MA1 MMW	2.65±0.21
aPA/SAN/MMA-MA5 MMW	2.75±0.07
aPA/SAN/MMA-MA10 MMW	3.00±0.14
aPA/SAN/MMA-MA1 LMW	3.00±0.14
aPA/SAN/MMA-MA5 LMW	2.90±0.14
aPA/SAN/MMA-MA10 LMW	2.95±0.07

Conclusions

The aPA/SAN blend, although thermodynamically immiscible, showed a phase morphology with small SAN disperse phase particles, due to the similarity of melt viscosity during the mixing. Morphological analysis of aPA/SAN/MMA-MA blends clearly showed that the increase in the concentration of MA groups in the MMA-MA copolymer increases the size of SAN disperse phase. Besides these morphological changes, indications that he interfacial tension may not be influenced by the compatibilizer characteristics studied in this work, such as the molecular weight and the amount of maleic anhydride, were displayed by the determination of the interface thickness by SAXS. These results show that the viscosity ration between the blends components is the main factor responsible by the formation of the phase morphology of the blends studied.

Acknowledgements. The authors want to thank DuPont and Dow Chemical by the materials donation, CNPq and FINEP/PRONEX by the financial support, Laboratório Nacional de Luz Síncroton by the SAXS measurements and Laboratório de Caracterização Estrutural (LCE) by

the MET measurements. We also thank Dr Nelson M. Larocca for the assistance with the SAXS measurements.

References

1. DR Paul, S Newman. Polymer Blends. V.1 e 2. New York: Academic Press, 2000.
2. K Wallheinke, W Heckmann, P Pötsschke, et al. Polymer testing, 1998;17:247.
3. EM Araújo, E Hage Jr., AJF Carvalho. Journal of applied polymer science, 2003;87:842.
4. J Roeder, RVB Oliveira, V Soldi, MC Gonçalves. ATN Pires. Polymer testing, 2002;21:815.
5. SP Jang, D Kim. Polymer engineering and science, 2000;40(7):1635.
6. K Cho, KH Seo, TO Ahn. Polymer journal, 1997; 29(12):987.
7. K Cho, KH Seo, TO Ahn. Journal of applied polymer science, 1998,68:1925-1933.
8. JS Chiou, DR Paul, JW Balow. Polymer, 1982;23:1543.
9. NM Larocca, E Hage Jr, LA Pessan. Journal of polymer science:Part B: Polymer physics, 2005;43:1244.
10. D Spridon, L Panaitescu, D Ursu, CV Uglea, I Popa, RM Ottenbrite. Polymer international, 1997;43: 175.
11. D Becker, E Hage Jr., LA Pessan. Journal of applied polymer science, 2007; 106(5):3248.
12. H-M Li, H-B Chen, Z-G Shen, S Lin. Polymer, 2002;43:5455.
13. VJ Triacca, S Ziaee, JW Barlow, et al. Polymer, 1991;32(8):1401.
14. AJ Oshinski, H Keskkula, DR Paul. Polymer, 1992;33(2):284.
15. BD Favis, JP Chalifoux. Polymer engineering and science, 1987;27(20):1591.
16. P Perrin, RE Prud´Homme. Macromolecules, 1994;27: 1852.
17. H Yu, A Natansohn, MA Singh, T Plivelic. Macromolecules, 1999;32:7562.
18. CG Vonk. Journal of applied crystallography, 1973;6:81.
19. JT Koberstein, B Morra, RS Stein. Journal of applied crystallography, 1980;13:34.